Load Voltage Control of a Wind Turbine-driven Three-phase Squirrel-Cage Induction Generator in an Islanded Microgrid

S. A. Kamilu[1,2*], L. Olatomiwa[3,4], O. M. Longe[4], S. Ikuforiji[2]

[1]Department of Power Mechatronics/Electrical Drives, Institute of Electrical Power Engineering and Energy Systems, 38678, Technische Universität Clausthal, Germany.
[2] Department of Electrical Engineering, Waziri Umaru Federal Polytechnic, Birnin Kebbi, 860262, Kebbi State, Nigeria.
[3]Department of Electrical and Electronics Engineering Federal University of Technology Minna, P.M.B. 65 Minna, Nigeria.
[4]Department of Electrical and Electronic Engineering Science, University of Johannesburg, Johannesburg 2006, South Africa.

ABSTRACT: The intermittent nature of the wind resources and reactive power consumptions are major issues associated with squirrel cage induction generator wind power system when operated in an island microgrid mode. The resultant effect of these two issues are continuous fluctuations of load voltage which has adverse effects on electrical devices. This paper proposes a voltage regulation technique based on proportional controller and phase deposition sine pulse width modulation (PDSPWM) for the control of 5-level neutral point clamped multilevel inverter. The instantaneous voltage tracking strategy based on root mean square value of microgrid voltage was adopted to regulate and maintain the output load voltage at 400 V_{rms} despite rotor fluctuations with wind speeds. The simulation was carried out in a MATLAB/SIMULINK environment and the performance of the control scheme was found to be excellent.

NOMENCLATURE

w = rotating speed of an arbitrary reference frame
w_r = rotor electrical angular speed
C_d, C_q = dq -axis self-excitation capacitances
p = derivative operators
i_{ds}, i_{qs} = stator currents in the dq axis of the SEIG
i_{dr}, i_{qr} = rotor currents (referred to stator) in the dq axis of the SEIG
P = number of pairs of poles
T_L = load torque
K_{dr}, K_{qr} = initial rotational induced voltages along dq axis
i_m = magnetizing current
J = Moment of inertia
V_{ds}, V_{qs} = stator voltages in the dq-axis of the SEIG
V_{dsc}, V_{qsc} = dq stator capacitor voltage
V_{dr}, V_{qr} = rotor voltages (referred to stator) in the dq axis of the SEIG
V_{dsc0}, V_{qsc0} = initial dq capacitor voltages
L_{ls}, L_{lr} = stator and rotor (referred to stator) leakage inductances of SEIG
L_s, L_r = stator and rotor (referred to stator) self-inductances of SEIG
L_m = magnetizing inductance
r_s, r_r = stator and rotor (referred to stator) resistance of SEIG
$\lambda_{ds}, \lambda_{qs}$ = stator flux linkages in the dq axis of the SEIG
$\lambda_{dr}, \lambda_{qr}$ = rotor flux linkages in the dq axis of the SEIG
T_e = electromagnetic torque of the SEIG
V_{Ldq} = Load voltage in dq axis
i_{Ldq} = Load current in dq axis

I. INTRODUCTION

In recent years, both industry and academics have given significant attentions to renewable energy research. The rationale behind this significant attention for renewable energy is due to the problems associated with the traditional method of power generation like the greenhouse gas emission, depletion of fossil fuel, increasing and fluctuating nature of oil prices (Calgan & Demirtas, 2021). Renewable Energy (RE) resources especially solar and wind are now in the fore front of replacing the conventional synchronous generation. The efforts of the U.S and South Korea among other countries to increase the percentage of electricity generation from solar and wind to 20% of the total energy production by 2030 is an indication that transition RE generation has come to stay (Mehrjoo *et al*., 2020; Yun & Hur, 2021).

Among the RE resources, wind power system has become a major contributor to the modern energy project but the intermittent nature of the wind resources is one of the major issues that affects its operational output (Yun & Hur, 2021). The three main configurations of wind generating systems in both literature and commercial wind markets are Squirrel cage induction generator (SCIG), Doubly Fed induction generator (DFIG), and Permanent magnet synchronous generator (PMSG) (Chitransh *et al*., 2021; Li & Chen, 2008). From the rotational speed range perspective, wind turbines can be categorized into fixed speed, limited variable speed, and variable speed. SCIG is usually classified as a fixed speed wind turbine, wound rotor induction generator as limited variable type while DFIG and PMSG are classified as complete variable speed wind turbine (Kadam & Kushare, 2012). Just like other

distributed natural resources, wind generating power systems can either be grid connected or operated as an islanded microgrid. The operation in an islanded mode for distribution generation grid level is allowed temporarily when failure occurs in the main grid system (Willenberg et al., 2020). More so, islanded microgrid mode becomes a better alternative where the cost of grid extension is excessively high or where the transmission lines have to pass through thick bushes where the network security cannot be guaranteed. From economic point of view, the cost of system installation and maintenance in standalone application is reduced and this directly translates to reduction in cost per kWhr of electricity sold to the consumers of rural communities (Kamilu & Mekhilef, 2019). Self-excited induction generators are most desirable for remote applications because they do not require an external supply to produce the excitation magnetic field (El Akhrif et al., 2016). In order to properly excite SCIG, the capacitor bank of appropriate value must be connected across its terminals, the effect of magnetic saturation is necessary, and the inherent magnetic flux in the airgap of the machine must also be accounted for. The different methodologies for selecting appropriate excitation capacitance have been discussed in several literature (Goyal & Palwalia, 2016; Mahato et al., 2006; Silva et al., 2020). The issues limiting the use of SCIG for wind application are the reactive power consumption and poor voltage and frequency regulations under varying loads. The steady state condition of the generated voltage is not fixed but depends on the suitable combination of excitation capacitance, rotor speed and connected load at any time. Excitation capacitance can be fixed but the amount of load and the wind speed that invariably impacts on the generator speed are random in nature and thereby causes flickering of voltage, which could be disastrous to sensitive loads like electronic devices. When capacitive excitations is adopted, and the operation of SCIG in the linear region of magnetizing curve is desired, then the precise leading current has to be supplied in order to maintain voltage stability with varying loads of different power factor. Different controllers have been proposed in literature for reactive power compensation of SCIG. One of the most famous controllers is the static var compensator (SVC) (Çalgan et al., 2020). The SVC is composed of a thyristor-controlled reactor with a fixed or switched shunt capacitor. It regulates the voltage at its terminals by controlling the amount of reactive power injected into or absorbed from the power system. The control technique of the SVC uses three per phase connected capacitor, which are continuously being adjusted, and the effective capacitance of the SVC is controlled by changing the firing angle of the thyristors between fully conducting and non- conducting states (Zine-Eddine et al., 2018). However, direct capacitor switching is not convenient because excessive current surges occur at the switching instant and could inject lower order harmonics into the generator winding, which may cause excessive heating and consequently leading to the failure of the machine. Another drawback of SVC scheme is if proper control cannot be achieved during voltage dips, it can cause temporary demagnetization of SCIG. Recent researches are now drifting towards voltage cource converter (VSC) based reactive power compensation. In (Tischer et al., 2015), a three-

wire hybrid topology of switchable capacitor banks and distribution static compensator (DSTATCOM) for VSC was presented. The use of electronic controller (ELC) for voltage and frequency control of SCIG have also been presented in (Mishra & Tiwari, 2016; Murthy et al., 2006). Similar procedure of using STATCOM for voltage and frequency regulation via proportional integral (PI), Integrator proportional (IP), and reference signal tracking (RST) controllers have also been presented (Benghanem et al., 2013; Bouzid et al., 2015).

This paper discusses a technique based on neutral point clamped multilevel inverter (NPC-ML) with a simple proportional integral (PI) controller in conjunction with sine pulse width modulation (SPWM) control scheme to maintain and regulate the output load voltage at 400 Vrms. The inverter performance is influenced by switching strategy, and relate to output voltage harmonic content. There are numbers of inverter switching control techniques, but phase deposition sinusoidal pulse width modulation (PDSPWM) technique has been adopted in this paper. The modulation index generated by the PI controller was used to multiply the low frequency sinusoidal modulating signal before being compared with carrier signal of 10-kHz to generate the gate control signal for the Insulated-gate bipolar transistors (IGBTs).

II. SYSTEM CONFIGURATION AND CONTROL STRATEGY

Figure 1 shows the configuration of the proposed system. It is made up of a three phase SCIG driven by wind turbine via a mechanical transmission device that is incorporated to step up the slow rotational speed of the turbine rotor and provide the necessary shaft power needed to drive the generator to near rated synchronous speed of the machine (Sousa et al., 2001). Each phase of the stator winding is shunted with a right valued capacitor, C_{ex} to aid in the excitation process. An ideal rectifier is also provided to help in converting DC to AC while the voltage regulation is achieved through NPC-ML inverter. The inductance capacitance (LC) filter is needed to remove the harmonics present in inverter output before being passed to the load.

III. DYNAMIC MODELLING OF SEIG WITH LOAD

The model of SCIG is presented using d-q model in arbitrary reference frame. direct-quadrature (d-q) model is very effective in analyzing the transient and steady state conditions of any system dynamics with reduced number of computations and with complete solutions (Seyoum, 2003). The classical representation of induction machine is shown in Figure 2 while the equivalent circuit on load is shown in Figure 3. The classical d-q model of SCIG typically constitutes three sets of equations: voltage equations, flux equations, and motion equation.

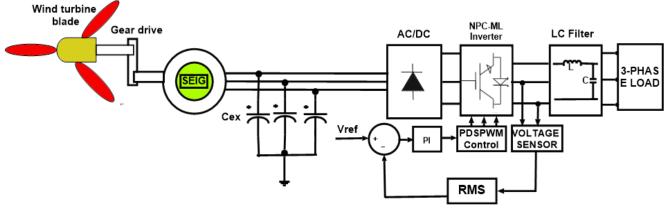The expression of these equations in an arbitrary reference frame are derived as follows;

Voltage equations:

$$V_{qs} = i_{qs}r_s + p\lambda_{qs} + w\lambda_{ds} \qquad (1)$$

$$V_{ds} = i_{ds}r_s + p\lambda_{ds} - w\lambda_{qs} \qquad (2)$$

$$V_{qr} = i_{qr}r_r + p\lambda_{qr} + (w - \omega_r)\lambda_{dr} \qquad (3)$$

$$V_{dr} = i_{dr}r_r + p\lambda_{dr} - (w - \omega_r)\lambda_{qr} \qquad (4)$$

Figure 1: Schematic diagram of SEIG wind turbine driven voltage regulation system.
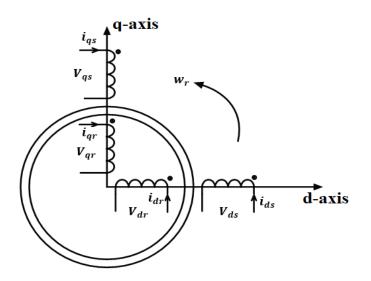

Figure 2: d-q representation of induction machine.

d-q flux linkages:

$$\lambda_{qs} = L_s i_{qs} + L_m i_{qr} \tag{5}$$
$$\lambda_{ds} = L_s i_{ds} + L_m i_{dr} \tag{6}$$
$$\lambda_{qr} = L_r i_{qr} + L_m i_{qs} \tag{7}$$
$$\lambda_{dr} = L_r i_{dr} + L_m i_{ds} \tag{8}$$

Where;

$$\begin{cases} L_s = L_{ls} + L_m \\ L_r = L_{lr} + L_m \end{cases} \tag{9}$$

Motion equations which describe the dynamic behavior of the rotor's speed in terms of mechanical and electromagnetic torque are jointly given in (10) (Khan *et al.*, 2022).

$$\begin{cases} \frac{2J}{P} p w_r = T_L - T_e - B_m w_r \\ T_e = \frac{3PL_m}{2}(i_{qs} i_{dr} - i_s i_{qr}) \end{cases} \tag{10}$$

Eqns. (11) and (12) were established considering the initial conditions of initial voltage on the excitation capacitors and remnant flux in the airgap (Sanusi *et al.*, 2021).

$$\begin{cases} V_{qsc} = \frac{1}{c_q} \int i_{qs}\, dt + V_{qsc0} \\ V_{dsc} = \frac{1}{c_d} \int i_{qs}\, dt + V_{dsc0} \end{cases} \tag{11}$$

$$\begin{cases} w_r \lambda_{qr} = (L_r i_{qr} + L_m i_{qs}) + K_{qr} \\ w_r \lambda_{dr} = (L_r i_{dr} + L_m i_{ds}) + K_{dr} \end{cases} \tag{12}$$

Resistance inductance capacitance (RLC) load model is given in (13) (Simoes & Farret, 2007):

$$\begin{cases} V_{Ldq} = \frac{1}{C} \int i_{Cdq}\, dt = \frac{1}{C}\int (i_{dq} - i_{Ldq})\, dt \\ i_{Ldq} = \frac{1}{L}\int (V_{Ldq} - R i_{Ldq})\, dt \end{cases} \tag{13}$$

To derive d-q model of SCIG in synchronous reference frame or stationary reference frame, w in the voltage equations is set to w_s and 0, respectively. Stationary reference frame is considered in the analysis of this paper. Also, since the rotor is short-circuited, it means $V_{dr} = V_{qr} = 0$. By also considering Eqn. (11), Eqns. (1) – (4) can be formulated in a state space form as given in (14).

$$\begin{bmatrix} L_s & 0 & L_m & 0 \\ 0 & L_s & 0 & L_m \\ L_m & 0 & L_r & 0 \\ 0 & L_m & 0 & L_r \end{bmatrix} \begin{bmatrix} pi_{qs} \\ pi_{ds} \\ pi_{qr} \\ pi_{dr} \end{bmatrix} +$$

$$\begin{bmatrix} r_s & 0 & 0 & 0 \\ 0 & r_s & 0 & 0 \\ 0 & -w_r L_m & r_r & -w_r L_r \\ w_r L_m & 0 & w_r L_r & r_r \end{bmatrix} \begin{bmatrix} i_{qs} \\ i_{ds} \\ i_{qr} \\ i_{dr} \end{bmatrix} + \begin{bmatrix} V_{qsc} \\ V_{dsc} \\ K_{qr} \\ K_{dr} \end{bmatrix} = \begin{bmatrix} 0 \\ 0 \\ 0 \\ 0 \end{bmatrix} \tag{14}$$

The matrix of the current vectors derivatives is obtained and given in (15).

$$\begin{bmatrix} pi_{qs} \\ pi_{ds} \\ pi_{qr} \\ pi_{dr} \end{bmatrix} =$$

$$\frac{1}{L_r L_s - L_m^2}\left(\begin{bmatrix} -L_r r_s & -L_m^2 w_r & L_m r_r & -w_r L_m L_r \\ L_m^2 w_r & -L_s r_s & w_r L_m L_r & L_m r_r \\ L_m r_s & w_r L_m L_s & -L_s r_r & w_r L_s L_r \\ -w_r L_m L_s & L_m r_s & -w_r L_r L_s & -L_s r_r \end{bmatrix} \begin{bmatrix} i_{qs} \\ i_{ds} \\ i_{qr} \\ i_{dr} \end{bmatrix} + \begin{bmatrix} L_m K_{qr} - L_r V_{qsc} \\ L_m K_{dr} - L_r V_{dsc} \\ L_m V_{qsc} - L_s K_{qr} \\ L_m V_{dsc} - L_r K_{dr} \end{bmatrix} \right) \tag{15}$$

Using least square curve fit, the magnetizing inductance, L_m is expressed as a function of the magnetizing current i_m and given in (16) (Simoes & Farret, 2007);

$$L_m = 0.423e^{-0.0035i_m^2} + 0.0236 \tag{16}$$

Figure 3: Equivalent circuit of capacitive SEIG in stationary reference frame.

Magnetizing curve of SCIG is nonlinear caused by saturation of the core, therefore L_m is not constant but rather depends on the instantaneous value of the magnetizing current i_m, which is evaluated in each step of the integration and given in (17) (Mahato *et al.*, 2013).

$$i_m = \sqrt{\frac{(i_{ds}+i_{dr})^2+(i_{qs}+i_{qr})^2}{2}} \tag{17}$$

IV. MODELLING OF WIND TURBINE AND THE GEAR DRIVE

The amount of aerodynamic power, P_m extractable from the wind of mean velocity, v_w, air density, ρ and flowing towards rotor blades of swept area, A is given by (18) (Makewita, 2022). The mechanical torque developed by the wind turbine, T_m, and the tip speed ratio (λ) of the wind turbine are given in Eqn. (19);

$$P_m = \frac{1}{2}\rho A v_w^3 C_p(\lambda,\beta) \tag{18}$$

$$\begin{cases} T_m = \frac{P_m}{w_t} \\ \lambda = \frac{w_t R}{v_w} \end{cases} \tag{19}$$

Where R is the turbine radius and w_t is the angular velocity (rad/sec) of the turbine. There are numbers of fitted equations for power coefficient, C_p, but a more generic one is given in (20) (Eltamaly *et al.*, 2013):

$$\begin{cases} C_p(\lambda,\beta) = 0.5176\left\{\left(\frac{116}{\lambda_i}\right) - 0.4\beta - 5\right\}e^{-\frac{21}{\lambda_i}} + 0.0068\lambda \\ \qquad where\ \lambda_i = \frac{1}{\lambda + 0.08\beta} - \frac{0.035}{1+\beta^3} \end{cases} \tag{20}$$

The pitch angle, β was set to zero for optimum aerodynamic power efficiency. Gear train is important in wind energy conversions due to the slow rotation of wind turbine rotor at low wind speed. The use of drive train also reduces the weight of nac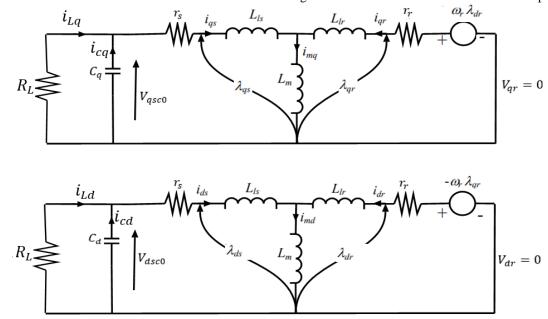elle and the sizes of the tower and plinth (Nejad *et al.*, 2022). In this paper, two mass model is considered. Figure 4 shows the schematic of two mass drive train. The turbine self-damping (D_t) is the aerodynamic resistance in the turbine blade and the generator self-damping (D_g) denotes mechanical friction and the windage.

The mutual damping (D_m) is the balancing dynamics that arise as a result of different speeds between the generator rotor and the turbine shaft. Turbine and generator self-damping can be neglected and the resulting mathematical models are given in (21) (David, 2010; Kabat *et al.*, 2022).

$$\begin{cases} \frac{dw_t}{dt} = \frac{1}{2H_t}(T_m - T_e) \\ \frac{1}{w_{ebs}}\frac{d(\theta_t-\theta_r)}{dt} = w_t - w_r \\ T_e = K_s(\theta_t - \theta_r) + D_t\frac{d(\theta_t-\theta_r)}{dt} \end{cases} \tag{21}$$

Where; H_t is the Inertia constant () of the turbine, K_s is the Stiffness constant; w_t and w_r are turbine and generator rotor speeds in per units (pu); θ_t and θ_r are turbine and generator angular displacements in rads; T_m and T_e (pu) are turbine input torque and generator torques, respectively.

V. CONTROL SCHEME FOR CONSTANT LOAD VOLTAGE CONTROL

Root mean square (RMS) voltage tracking is implemented to study the steady state stability and voltage dip condition of the load voltage. It does include all components like: harmonics, inter-harmonics e.t.c (Tarasiuk, 2015). Usually, when it is necessary to evaluate the performance of connected loads in power system network only RMS electrical quantities are used (Hossain & Pota, 2015).

Figure 4: Two-mass drive train model of a wind turbine.

Figure 5 illustrates the SIMULINK model of the proposed control scheme. To generate appropriate modulation index necessary for the voltage control, the gains of the PI controller $(i.e., K_p$ and $K_i)$ were obtained using heuristic tuning method, i.e., the Ziegler–Nichols method. The modulation index, m is then used in conjunction with PDSPWM scheme to generate the switching pulses.

VI. RESULTS AND DISCUSSION

The simulation results using MATLAB/SIMULINK software, version R2020b were presented. The voltage at the direct output terminals of SCIG and NPC-ML were first

simulated at wind speed of 10m/s, an excitation capacitance of $100 - \mu F$, and resistive load of 500 Ω to serve as a pre-test for the entire system. The results are as depicted in Figures 6 and 7.

Before the constant output voltage control action of the DC/AC inverter was incorporated, it was also necessary to first simulate the microgrid with varying wind speed and varying loads to examine their impacts on certain parameters of the machine (see Figure 8). Any step increases in wind speed results in corresponding step increase in generator rotor speeds, as shown in Figures 8 (a) and (b).
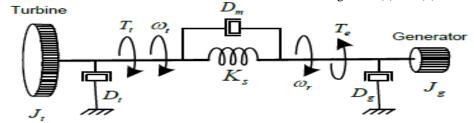
It is necessary that electromagnetic torque and mechanical torque are equal and opposite for stability reasons, and that has been achieved as illustrated in Figures 8 (c) and (d). The effects of varying wind speed on the microgrid with a fixed load resistance of 500 ohms was simulated without the control scheme as shown in Figure 9 and with the voltage control scheme as illustrated in Figure 10.
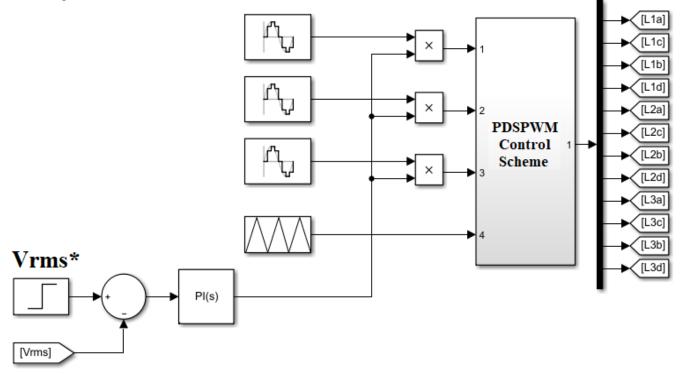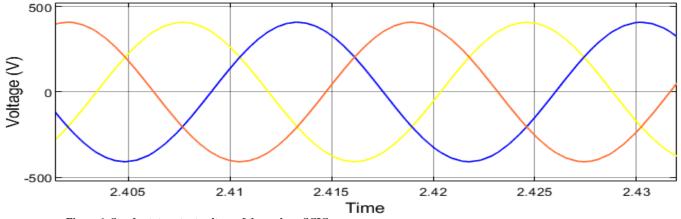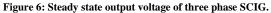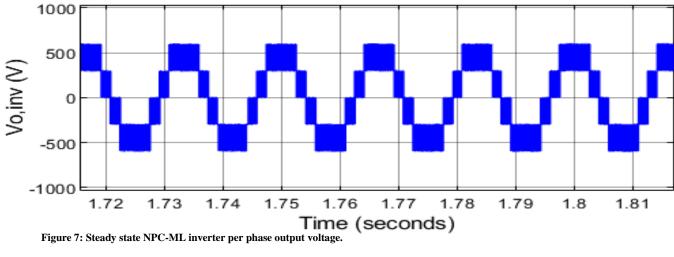

Figure 5: Control scheme for constant load voltage control.

Figure 6: Steady state output voltage of three phase SCIG.

Figure 7: Steady state NPC-ML inverter per phase output voltage.

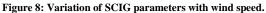**Figure 8: Variation of SCIG parameters with wind speed.**

Figure 9 demonstrates variations in both inverter output voltage and the SCIG rotor speed in direct correspondence with the variations in wind speed. Meanwhile, with the incorporation of the constant voltage control scheme, load voltage remains constant with wind speed fluctuations (see Figure 10).

depicted in Figure 11, with the Figure 11 (a) showing how the wind speed was kept constant at 10 m/s.

Now, when the constant voltage control was incorporated, the output load voltage was kept constant at a set value of 400
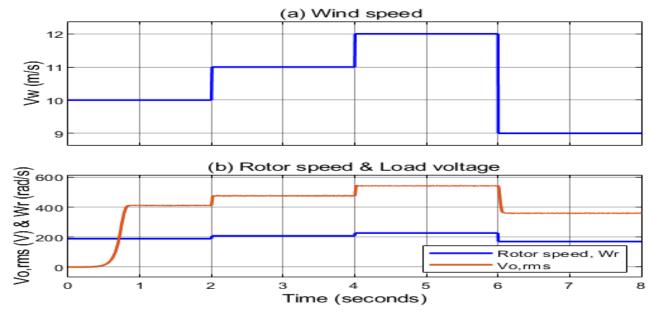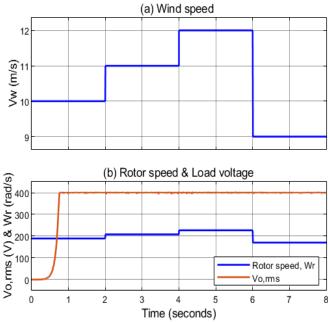

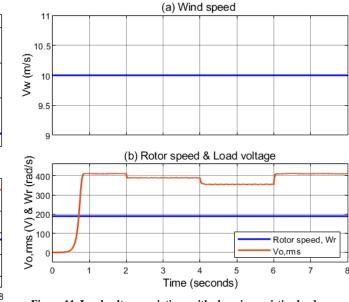**Figure 9: Effect of wind speed variation on the load voltage, RL at 500 ohms.**

Figure 10: Load voltage regulation with fluctuating wind speed.

Figure 11. Load voltage variations with changing resistive loads, $V_w = 10m/s$.

To simulate the effect of load variations on microgrid voltage, set of load impedances were switched on to the SCIG in parallel at specific time intervals so that subsequent equivalent impedance kept decreasing e.g $R_L = (500, 120, 120)\Omega$ at $t = (0, 2, 4)\ seconds$. At exactly 6 sec., the two added loads of 120 Ω were removed so that the system is returned to an initial load of 500 Ω. The sequence of the described load variations is as

The V_{rms} (as shown in Figure 12), this does demonstrate the robustness of the control scheme, though at critical value of generator speed and load, the machine excitation would collapse. To demonstrate the voltage collapse phenomenon in SCIG, resistive loads were switched on in parallel in the sequence $R_L = (500, 250, 20)\Omega$ at $t = (0, 5, 10)\ seconds$. Figure 13 illustrates the demagnetization phenomenon.
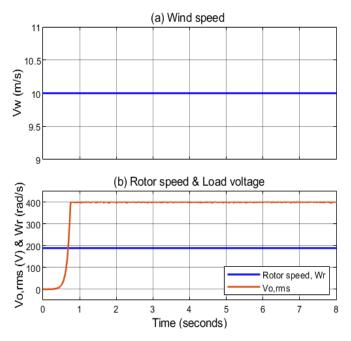
Figure 12. Load voltage regulation with changing resistive loads, $V_w = 10$ m/s.
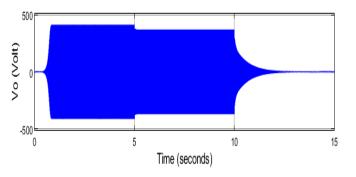

Figure 13: Voltage collapse phenomenon at extreme load condition.

VII. CONCLUSIONS

This paper examined the proposed technique to control the load voltage of an islanded microgrid for three phase SEIG driven by a wind turbine. Comprehensive modelling of SEIG and wind turbine with 2-mass drive train has been presented. A 5-level neutral point clamped multilevel inverter (NPC-ML) inverter that generates a sinusoidal-like voltage was used to interface SCIG with the grid so that small filter size is required. The constant voltage control scheme was realized using a PI controller which produces a varying modulation index that ensures the error between the sensed RMS load voltage and the set value is brought to zero. The instantaneous voltage tracking strategy based on RMS value of microgrid voltage was implemented to study the steady state stability and dip condition under varying wind speed and impedance load. The controller performance was found to be effective as no traceable error was observed.

AUTHOR CONTRIBUTIONS

It was all a joint work all through from the beginning to the end. The main research idea was initially conceptualized

by **S.A. Kamilu** while the creation of the models, review and writing of the original draft were carried out jointly. Software validation of the developed model was carried out by **S.A. Kamilu** and **L. Olatomiwa** and the confirmation for possible errors was then carried out by **O.M. Longe** and **I. Solomon**. The revision of the paper was carried out by **S.A. Kamilu** and **L. Olatomiwa**. **S.A. Kamilu** coordinated the whole research work.

REFERENCES

Benghanem, M.; A. Bouzid; M. Bouhamida and A. Draou. (2013). Voltage control of an isolated self-excited induction generator using static synchronous compensator. Journal of Renewable and Sustainable Energy, 5(4), 043118.

Bouzid, A. M.; P. Sicard; A. Cheriti; J. M. Guerrero; M. Bouhamida and M. S. Golsorkhi. (2015). Voltage and frequency control of wind-powered islanded microgrids based on induction generator and STATCOM. Paper presented at the 2015 3rd International Conference on Control, Engineering & Information Technology (CEIT).

Calgan, H. and Demirtas M. (2021). A robust LQR-FOPIλDµ controller design for output voltage regulation of stand-alone self-excited induction generator. Electric Power Systems Research, 196, 107175.

Çalgan, H.; E. Ilten and M. Demirtas. (2020). Thyristor controlled reactor-based voltage and frequency regulation of a three-phase self-excited induction generator feeding unbalanced load. International Transactions on Electrical Energy Systems, 30(6), e12387.

Chitransh, A.; S. Kaur and R. Parveen. (2021). Comparative analysis of different configuration of generators for extraction of wind energy. Paper presented at the 2021 Fifth International Conference on I-SMAC (IoT in Social, Mobile, Analytics and Cloud)(I-SMAC).

David, P. P. (2010). Sustainable Power Production and Transportation. Assignment II. Chalmers University of Technology, Sweden. Retrieved from https://www.google.com.my/?gws_rd=cr,ssl&ei=YrFHVLztC czauQShhICoAQ#q=sustainable+power+production+and+tra nsportation+by+Peiyuan+Poopak+David

El Akhrif, R.; A. Abbou; M. Barara and Y. Majdoub. (2016). Modeling and simulation for a three-phase voltage source inverter using a self-excited induction generator. Paper presented at the 2016, 7th International Renewable Energy Congress (IREC).

Eltamaly, A. M.; A. Alolah and H. M. Farh. (2013). Maximum Power Extraction from Utility-Interfaced Wind Turbines. New Developments in Renewable Energy, pp.159-192.

Goyal, S. K. and Palwalia D. (2016). Analysis of performance parameters and estimation of optimum capacitance for asynchronous generator. Engineering Science and Technology, an International Journal, 19(4), 1753-1762.

Hossain, M. A. and Pota. H.R. (2015). Voltage tracking of a single-phase inverter in an islanded microgrid. International Journal of Renewable Energy Research, 5(3), 806-814.

Kabat, S. R.; C. K. Panigrahi; B. P. Ganthia; S. K. Barik and B. Nayak. (2022). Implementation and Analysis of Mathematical Modeled Drive Train System in Type III Wind

Turbines Using Computational Fluid Dynamics. Advances in Science and Technology Research Journal, 16(1), 180-189.

Kadam, D. and Kushare B. (2012). Overview of different wind generator systems and their comparisons. International journal of engineering science & advanced technology, 2(4), 1076-1081.

Kamilu, S. and Mekhilef. S (2019). Three phase grid connected Neutral Point Clamped (NPC) multilevel inverter fed by two wind turbines. Pertanika Journal of Science and Technology, 27 (4): 2173 - 2187.

Khan, M. F.; M. R. Khan and A. Iqbal. (2022). Effects of induction machine parameters on its performance as a standalone self-excited induction generator. Energy Reports, 8, 2302-2313.

Li, H. and Chen Z. (2008). Overview of different wind generator systems and their comparisons. IET Renewable Power Generation, 2(2), 123-138.

Mahato, S.; M. Sharma and S. Singh. (2006). Determination of minimum and maximum capacitances of a self-regulated self-excited single-phase induction generator using a three-phase winding. Paper presented at the 2006 India International Conference on Power Electronics.

Mahato, S.; S. Singh and M. Sharma. (2013). Dynamic behavior of a single-phase self-excited induction generator using a three-phase machine feeding single-phase dynamic load. International Journal of Electrical Power & Energy Systems, 47, 1-12.

Makewita, L. D. (2022). Wind Farm Modeling in DIgSILENT PowerFactory® and Load Flow Analysis of Internal Collector Network. (MSc dissertation, Department of Earth Sciences, Uppsala University, Sweden).

Mehrjoo, M.; M. J. Jozani and M. Pawlak. (2020). Wind turbine power curve modeling for reliable power prediction using monotonic regression. Renewable Energy, 147, 214-222.

Mishra, E. and Tiwari S. (2016). Fuzzy logic control based electronic load controller for self-excited induction generator. Paper presented at the 2016 International Conference on Electrical Power and Energy Systems (ICEPES).

Murthy, S.; M. Gayathri; K. Naidu and U. Siva. (2006). A novel digital control technique of electronic load controller for SEIG based micro hydel power generation. Paper presented at the 2006 International Conference on Power Electronic, Drives and Energy Systems.

Nejad, A. R.; J. Keller; Y. Guo; S. Sheng; H. Polinder; S. Watson; J. Dong; Z. Qin; A. Ebrahimi and R. Schelenz.

(2022). Wind turbine drivetrains: state-of-the-art technologies and future development trends. Wind Energy Science, 7(1), 387-411.

Sanusi, A. K., Olatomiwa, L., Mohammed, A., & Sodiq, K. (2022). Capacitively-excited single-phase asynchronous generator for autonomous applications. Nigerian Journal of Technological Development, 19(2), 128-135.

Seyoum, D. (2003). The dynamic analysis and control of a self-excited induction generator driven by a wind turbine. University of New South Wales. (Doctoral dissertation, University of New South Wales, Sydney).

Silva, E. O.; W. E. Vanço and G. C. Guimarães. (2020). Capacitor bank sizing for squirrel cage induction generators operating in distributed systems. IEEE Access, 8, 27507-27515.

Simoes, M. G. and Farret F.A. (2007). Alternative energy systems: design and analysis with induction generators (Vol. 13): CRC press.

Sousa, G. C.; F. N. Martins; J. P. Rey and J. A. Bruinsma. (2001). An autonomous induction generator system with voltage regulation. Paper presented at the 4th IEEE International Conference on Power Electronics and Drive Systems. IEEE PEDS 2001-Indonesia. Proceedings (Cat. No. 01TH8594).

Tarasiuk, T. (2015). Comparative study on chosen methods of voltage dip tracking based on real example. Paper presented at the XXI IMEKO World Congress "Measurement in Research and Industry" August.

Tischer, C. B.; L. G. Scherer and R. F. de Camargo. (2015). Voltage and frequency regulation of induction generator based system applying proportional-resonant controller. Paper presented at the 2015 IEEE 13th Brazilian Power Electronics Conference and 1st Southern Power Electronics Conference (COBEP/SPEC).

Willenberg, D.; A. Winkens and P. Linnartz. (2020). Impact of wind turbine generator technologies and frequency controls on the stable operation of medium voltage islanded microgrids. Electric Power Systems Research, 189, 106760.

Yun, E. and Hur J. (2021). Probabilistic estimation model of power curve to enhance power output forecasting of wind generating resources. Energy, 223, 120000.

Zine-Eddine, B. T.; N. Ali; M. Said and I. Rachid. (2018). A New Control Method of Three-Phase Self Excited Induction Generator Feeding Single-Phase Load by using Static Var Compensator. Paper presented at the 2018 International Conference on Wind Energy and Applications in Algeria (ICWEAA).